Bull Volcanol (2013) 75:758
DOI 10.1007/s00445-013-0758-6

COLLECTION: MONOGENETIC VOLCANISM

Space–time evolution of monogenetic volcanism in the mafic Garrotxa Volcanic Field (NE Iberian Peninsula)

C. Cimarelli · F. Di Traglia · D. de Rita · D. Gimeno Torrente · J-. L. Fernandez Turiel

Received: 14 December 2012 / Accepted: 3 September 2013 / Published online: 8 October 2013

Abstract We reconstructed the evolution of the volcanic activity within the central Garrotxa monogenetic Volcanic Field, the youngest volcanic area of the Iberian Peninsula, by investigating the stratigraphy of the volcanic successions and the morphology of the monogenetic eruptive centres. Analysis of this volcanic succession has been conducted following the Unconformity Bounded Stratigraphic Units criteria. The detailed stratigraphy of the volcanic successions shows that the central Garrotxa Volcanic Field (GVF) evolved through four main periods of volcanic activity (Synthems) represented by the eruptive products of the mafic monogenetic volcanoes and associated syn-eruptive reworked deposits (Eruptive Units) and by the inter-eruptive deposits (Epiclastic Units). The distribution and the morphologies of the monogenetic volcanoes suggest that feeder dykes were emplaced under influence of the present stress filed and along pre-existing fractures of the basement. Our facies analysis of the deposits and their distribution shows that migration of volcanism toward the centre of the basin was accompanied by a trend of increasing explosivity. Episodic hydromagmatism in central Garrotxa occurred without a specific geographic locus or obvious temporal correlation. Finally, by integrating field data with the stratigraphy extracted from water wells, we determined the volume of the volcanic deposits. The small average volume of products emitted during each eruptive period, and the long quiescence separating them, allow us to classify the GVF as a low-output rate volcanic field.

Keywords Garrotxa · Mafic volcanic field · Scoria cone · Monogenetic · UBSU

Introduction

Volcanic fields in continental settings commonly consist of scattered or closely spaced small volcanoes, mostly mafic in composition. These volcanoes are often referred to as

Editorial responsibility: I.E.M. Smith, Guest Editor

This paper constitutes part of a topical collection:

Smith IEM, Nemeth K, and Ross P-S (eds) Monogenetic volcanism and its relevance to the evolution of volcanic fields.

C. Cimarelli (✉)
Department of Earth and Environmental Sciences,
Ludwig-Maximilians-Universität München,
Theresienstraße 41, 80333 Munich, Germany
e-mail: cimarelli@min.uni-muenchen.de

F. Di Traglia
Department of Earth Sciences, University of Pisa,
Via Santa Maria 53, Pisa, Italy
e-mail: federico.ditraglia@unifi.it

F. Di Traglia
Department of Earth Sciences, University of Firenze,
Via La Pira 4, Firenze, Italy

D. de Rita
Dipartimento di Scienze Geologiche, Università Roma Tre, L.go Murialdo 1, Roma, Italy
e-mail: derita@uniroma3.it

D. Gimeno Torrente
Department Geoquímica, Petrologia i Prospecció Geològica,
Universitat de Barcelona, Carrer Martí i Franquès s/n,
08028 Barcelona, Spain
e-mail: domingo.gimeno@ub.edu

J-. L. Fernandez Turiel
Institute of Earth Sciences "Jaume Almera," CSIC, Solè i Sabaris s/n,
08028 Barcelona, Spain
e-mail: jlfernandez@ictja.csic.es

monogenetic because it is believed that they erupt only once and their activity rapidly wanes (Walker 1993; Connor and Conway 2000; Valentine and Gregg 2008). They commonly form extensive cinder-cone fields, sometimes associated with polygenetic shield volcanoes (Tibaldi 1995; Corazzato and Tibaldi 2006; Dóniz et al. 2008).

The eruptive style of monogenetic basaltic volcanoes can change from Strombolian to Hawaiian to violent Strombolian in response to changing behaviour of the exsolving volatile species, magma rise-speed and the coupling between gas and melt plus crystals (Head and Wilson 1989; Parfitt 2004; Valentine and Gregg 2008; Cimarelli et al. 2010).

Monogenetic volcanism has been related to high regional differential stress, in areas with variable (high or low) magma input/output rate (Takada 1994). Low-output rate volcanic fields usually comprise a small number of widely spaced volcanoes (Valentine and Hirano 2010), while high-output rate volcanic fields comprise dense concentrations of cones, shields and surrounding lava plains (Condit and Connor 1996). The distribution of monogenetic volcanoes within basaltic volcanic fields is generally related to the geometry of the underlying magma source zone (Condit and Connor 1996; Valentine and Keating 2007; Kiyosugi et al. 2010) and/or to the presence of tectonic structures in the shallow crust (Valentine and Perry 2007; Keating et al. 2008).

The Garrotxa Volcanic Field (GVF), the most recent volcanic area in the Iberian Peninsula (0.5–0.01 Ma, Araña et al. 1983; Puiguriguer et al. 2012), consists of more than 40 well-preserved monogenetic centres, grouped in two different zones: (1) a central zone, where the younger cones are located (the central GVF) and (2) a peripheral zone that consists of about 12 widely scattered vents (Araña et al. 1983). Despite their fairly conical morphology, some of these edifices appear to have experienced a complex evolution with alternation of predominantly magmatic activity with minor phreatic and phreatomagmatic episodes (Di Traglia et al. 2009; Gisbert Pinto et al. 2009; Martí et al. 2011). The existing dates for lavas and one paleosol from the central GVF show that the volcanic activity in this sector occurred between 247±17 ka and 11.5±1.ky BP (Guérin et al. 1985; Puiguriguer et al. 2012). Unfortunately, the dated lavas were not placed within a detailed stratigraphic scheme, and this prevents a thorough reconstruction of the spatial–temporal variation of volcanic activity within the central GVF.

We investigated the relationship between eruptive styles and distribution of volcanoes through time within the central Garrotxa tectonic depression.

Detailed stratigraphic analysis and geological mapping of the area (scale 1:5,000) allows us to define multiple volcanic successions and their relative chronology. The facies analysis of the deposits helped us to infer the eruptive styles experienced by each volcanic centre. Volcano morphologies and their internal structures have also been examined by integrating field data and a digital elevation model (DEM) to understand the relation between volcanism and local/regional tectonics. Finally, complementing field data with water well stratigraphy, we were able to reconstruct the top surface of the pre-volcanic basement and to define the thickness and the total volume of the volcanic deposits. Combining the existing geochronology and the volume estimate we have been able to determine the total volcanic output rate in the central GVF.

Geological setting

Geodynamic significance of the North East Volcanic Province of Spain

The GVF is located about 90 km NNE of Barcelona and about 30 km NW of the city of Girona, in the pre-Pyrenees area (Fig. 1a). The GFV together with the Ampurdà (AVF), Tordera (TVF) and Selva (SVF, also called southern Garrotxa; Martí et al. 2011) volcanic fields is part of the North East Volcanic Province of the Iberian Peninsula (NEVP; Araña et al. 1983) also referred as the Catalan Volcanic Zone (Martí et al. 2011).

The Neogene to Quaternary NEVP volcanism is interpreted as the resulting from the Pyrenees post-collisional back–arc extension driven by the African slab retreat, which favoured the rise of magmas through the Iberian continental crust (Gallart et al. 1991; Zeyen et al. 1991; Martí et al. 1992). The NEVP volcanism is associated with a system of NE–SW and NW–SE regional faults that control the geometry of the main tectonic depressions in this area (Araña et al 1983). Volcanic activity in the NEVP took place between 10 and 0.01 Ma, with the oldest eruption in the AVF and the youngest in the GVF (Donville 1976; Araña et al. 1983). Migration of volcanism was coherent with the differential opening velocities of the western Mediterranean (Ligure–Provençal basin) during the Oligocene–Miocene, with its northern sector (Gulf of Lyons) experiencing a faster opening respect to the southern-most part (Valencia margin; Mauffret et al. 1995; Goula et al. 1999). In the same way, volcanism migrated from NE to SW. During the Pliocene–Lower Pleistocene, volcanism migrated to the NW toward the GVF in accordance with the change in the regional stress orientation from pure extensional (vertical σ1 and NW-SE σ3) to mainly strike-slip motions (vertical σ2 and NNW-SSE σ1; Goula et al. 1999). Westward migration of the extensional regime at a rate of 5 mm/year (Vergés and Sàbat 1999) and the consequent migration of volcanism is interpreted in terms of mechanical removal of the mantle lithosphere by buoyancy due to the migration of a thermally heterogeneous mantle (Cebrià et al. 2000). Such buoyancy is inferred to have caused regional scale doming of the crust centred on the tectonically and volcanically active region of the Garrotxa (Lewis et al. 2000).

NEVP parental magmas are petrologically similar to those feeding the Cenozoic to Quaternary intraplate volcanoes of central Europe (Massif Central, Provence Volcanic Field and

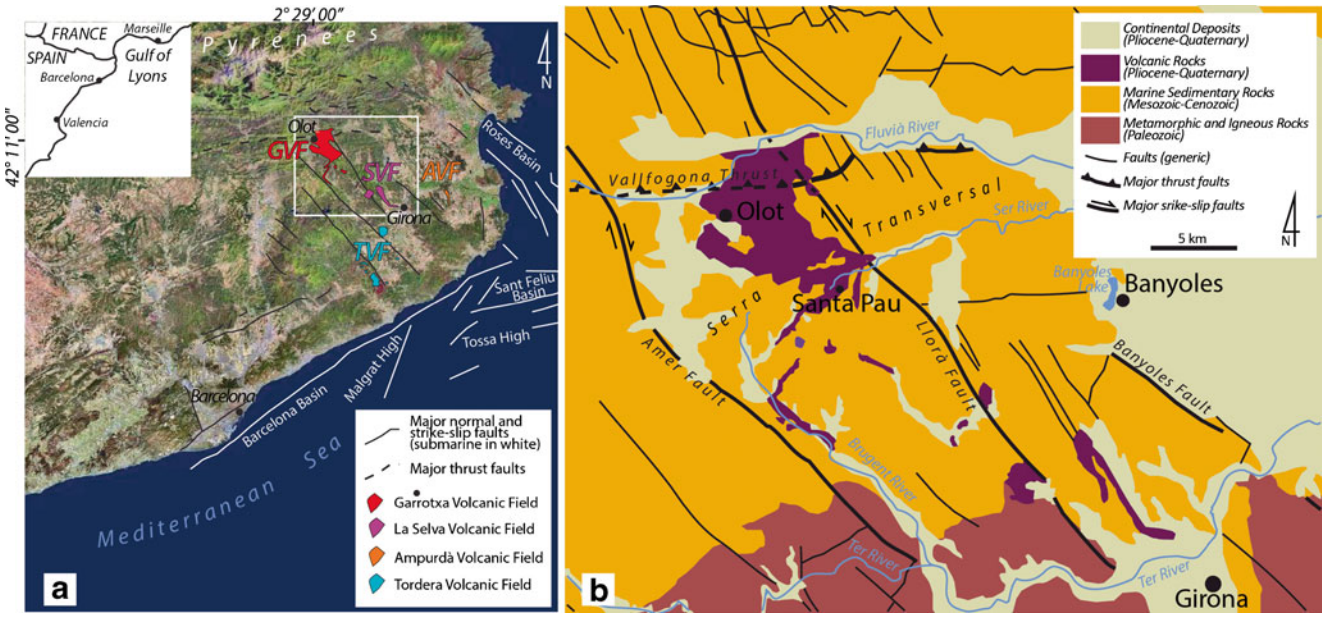

Fig. 1 **a** North-east Volcanic Province of Spain. *AVF*: Ampordà Volcanic Field; *TVF*: Tordera Volcanic Field; *SVF*: Selva Volcanic Field; *GVF*: Garrotxa Volcanic Field. Major structural lineaments on land and offshore are reported (after SGC Servei Geològic de Catalunya 1989 and Mauffret et al. 1995). **b** Schematic geological map of the GVF. Modified after SGC (1989)

Eifel Volcanic Field; Mertes and Schmincke 1985; Wilson et al. 1995; Bianchini et al. 2007; Carracedo Sánchez et al. 2012). Volcanic rocks from GVF include leucite basanites, nepheline basanites and alkali olivine basalts.

The pre-volcanic basement

The pre-volcanic basement in the central GVF consists of Paleozoic, Eocene and Quaternary rocks. Paleozoic units underlying the Eocene successions crop out south of the studied area and comprise mainly plutonic and metamorphic rocks (Fig. 1b). The Eocene succession in the Garrotxa area is made up of a deepening–shallowing set of nine depositional sequences broadly represented by alluvial systems capped by delta and shallow carbonate platform systems and finally evolving into a shallowing-upward succession characterised by evaporitic deposits followed by delta and alluvial systems (Gimenez-Monsant et al. 1999). These rocks have been extensively deformed and in the studied area they form E–W-oriented folds dissected by normal faults roughly parallel to their axes (Gallart et al. 1991; Gimenez-Monsant et al. 1999). The Quaternary sedimentary rocks consist of fluvial and lacustrine sediments and limited travertine deposits precedent and contemporaneous to the deposition of the volcanic products (IGC, 2002, 2003).

Two major NW-striking faults, the Amer fault to the west and the Llorà fault to the east, delimit the central Garrotxa tectonic depression. The tectonic depression is further delimited to the north and to the south by the Valfogona thrust and the sedimentary ridge of the Serra Transversal, respectively (Fig. 1b). The GVF is mainly localised in two different sectors of the tectonic depression: the Olot-Fluvià river valley to the north and the Santa Pau-Ser river valley to the south. Some of the major faults controlling the structural architecture of the area proved to be tectonically active in historical times, generating destructive earthquakes during the Middle Ages (Fleta et al. 2001).

The Unconformity Bounded Stratigraphic Units criteria

The fieldwork has been conducted following the Unconformity Bounded Stratigraphic Units criteria (UBSU; Salvador 1987, 1994), based on the hierarchy of the identified stratigraphic unconformities. The reference unit of the UBSU is the Synthem, defined as a stratigraphic body delimited by significant and demonstrable unconformities, preferably having a regional or inter-regional extension (Salvador 1987). Given the volcanic nature of the studied successions, we adopted the UBSU methodology modified for volcanic terrains (de Rita et al. 1997; Di Traglia et al. 2013). Within the framework of the UBSU, the Eruptive Unit (as defined by Fisher and Schmincke 1984) represents the basic lithostratigraphic unit within the Synthem (Fig. 2 for a general example). Different types of unconformities have been identified and classified according to their ranking (Fig. 3). Major unconformities (S1) extend over the whole studied area, characterised by diffuse areal erosion, and are marked locally by decimetre-thick paleosols. The S1 unconformities constitute the boundary of the different Synthems. Lower rank unconformities S2, locally corresponding to paleo-gullies, limit the Eruptive and Epiclastic Units within each Synthem.

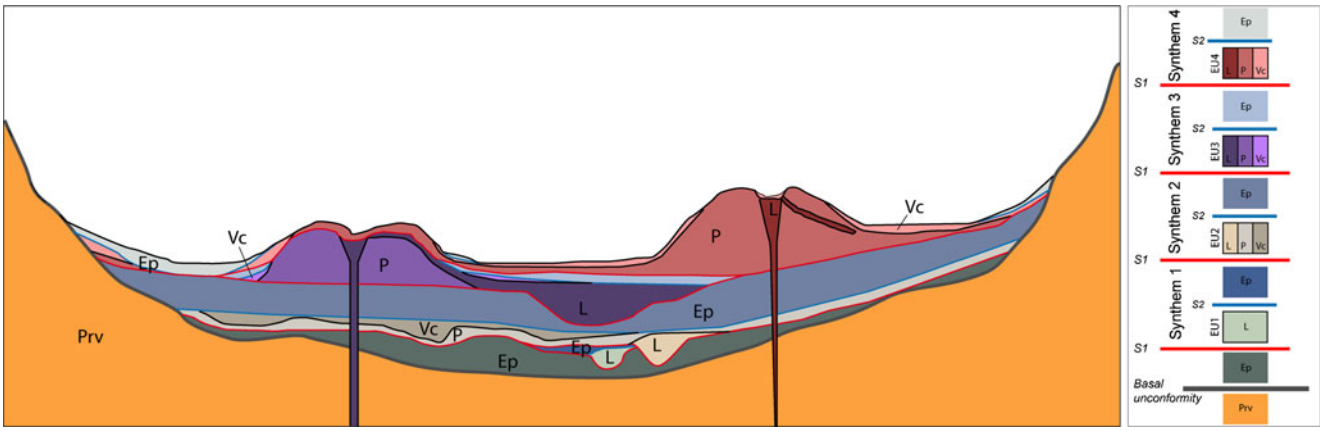

Fig. 2 Synthetic explanation of the UBSU methodology. The hypothetical cross-section shows the hierarchical relations between unconformity surfaces and the bounded stratigraphic units. A basal unconformity separates the pre-volcanic basement (*Prv*) from the volcanic deposits. Volcanic deposits are divided into four synthems separated by S1 unconformities (in *red*). Synthems are formed by primary volcanic deposits (lavas: *L*; and pyroclastic: *P*), their syn-eruptive volcaniclastic deposit (*Vc*) and by the epiclastic deposits (*Ep*) representing the inter-eruptive sedimentation. Primary and syn-eruptive volcanic deposits form the eruptive units (EU) and are separated by the epiclastic units (Ep) by lower hierarchy S2 unconformities (in *blue*)

Other smaller-scale unconformities (S3) are recognised within the Eruptive Units and separate primary (lavas and pyroclastic deposits) and/or syn-eruptive reworked deposits (see Figs. 3 and 4).

The study of about 50 stratigraphic sections (the more representative of which are sketched in Fig. 4) allowed us to make a geological map of the area (Fig. 5). Classification of the deposits is based on their lithological characteristics, average componentry of clasts and matrix, organisation and geometry and presence of sedimentary structures (Table 1), allowing distinction between primary and secondary deposits (Table 2).

Stratigraphy of the Central GVF

Volcanism in the Central GVF produced numerous small monogenetic eruptive centres aligned with the main structural features that controlled the evolution of the Central GVF tectonic depression. Volcanic activity was characterised by both effusive and explosive events that led to the emplacement of lava flows, lava sheets and construction of spatter cones and cinder cones.

Volcanic successions have been organised in four Synthems (Valls dels Arcs Synthem, Santa Pau Synthem, Mascou Synthem, Les Tries Synthem; Fig. 5, Table 1). In each

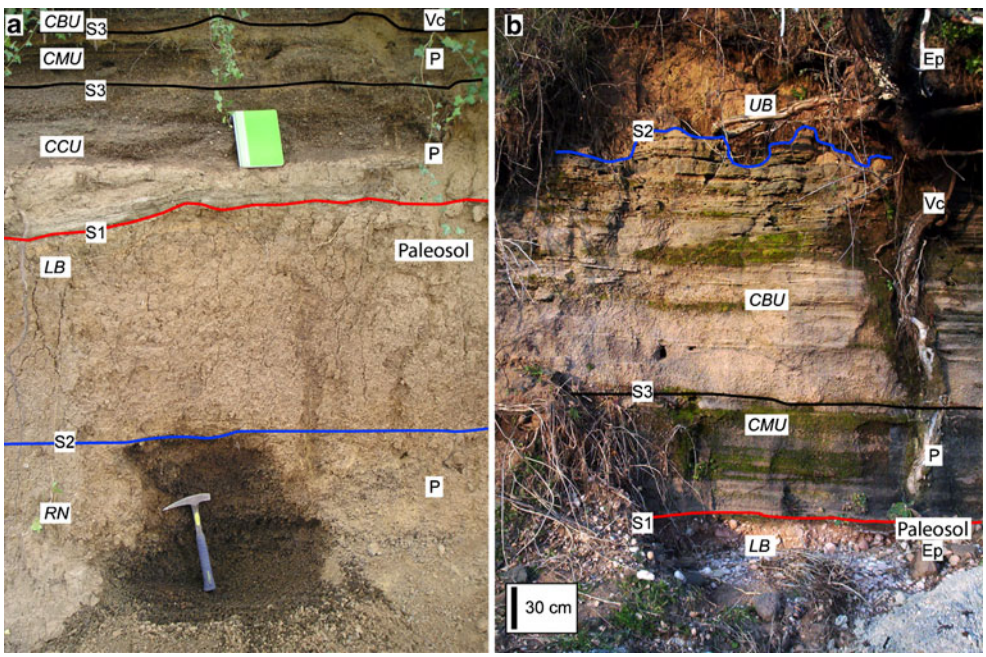

Fig. 3 Main stratigraphic log correlation of the central area of the GVF. The correlations allowed organising the volcanic successions into four synthems, separated by S1 unconformities of comparable hierarchy (*red lines*). Each Synthem is composed of one Eruptive Unit, in its turn composed of more than one eruptive episode, and of one Epiclastic Unit (limited by S2 unconformities: *blue lines*) representing inter-eruptive sedimentation

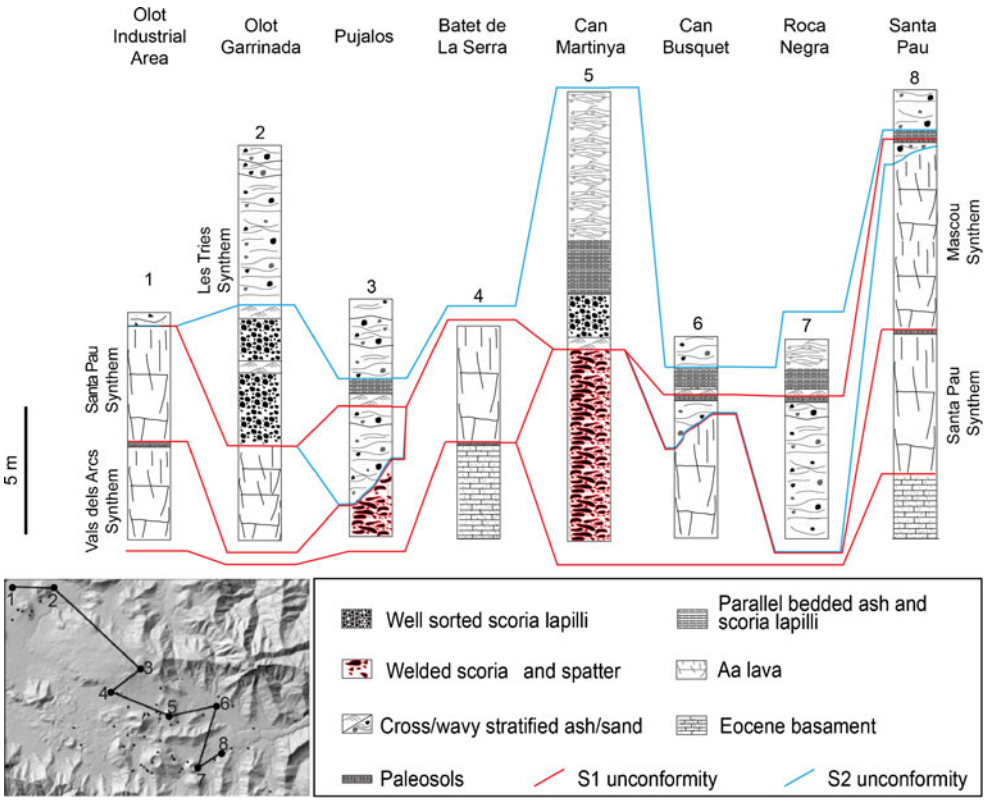

Fig. 4 Example of stratigraphic unconformities: **a** S1 unconformity between Mascou Synthem (*RN* and *LB* units) and Les Tries Synthem (*CCU, CMU* and *CBU* units). S2 unconformity lies between *RN* (pyroclastic deposits related to the Roca Negra scoria cone) and *LB* (epiclastic) units. **b** S1 unconformities between Mascou Synthem (*LB* unit) and Les Tries Synthem (*CMU, CBU* and *UB* unit). S2 unconformity lies between *CBU* (syn-eruptive reworking) and *UB* (epiclastic) units. Several lower-hierarchy unconformities (S3) lie between different pyroclastic deposits (*CCU*, *CMU*, *CBU*) within the same Croscat EU

Synthem, one Eruptive Unit (comprising both primary and syn-eruptive reworked deposits containing exclusively volcanic products, Figs. 4, 6 and Table 2) and one Epiclastic Unit (inter-eruptive deposits containing also non-volcanic sediments, Table 2) have been recognised. The three Epiclastic Units represent volcanically quiescent periods. The organisation of the studied successions in Synthems, according to the presence of unconformities of comparable hierarchy, indicates that the volcanism in the central GVF evolved through four main periods during which several eruptions (clusters) occurred, separated by comparable unconformities (i.e. comparable pauses in volcanic activity).

Facies analysis and eruptive style of volcanic centres

Facies analysis of the volcanic deposits allowed us to identify the eruptive styles of the volcanoes, and the transport and sedimentation mechanisms of primary and reworked pyroclastic material. A detailed description of the deposits is given in Table 1. From the facies analysis of the volcanic successions belonging to each eruptive unit, it is possible to reconstruct the eruptive style of each volcanic centre in the central GVF. In general, volcanic activity changed from mainly effusive to prevalently explosive through time. In fact, older eruptive units (Batet de La Serra EU and Puig de Mar EU, Fig. 6) were mainly characterised by the effusion of large lava sheets and lava flows through eruptive fissures. The explosive activity recorded in these early eruptions consisted of localised episodes of Hawaiian-type lava fountaining that constructed spatter ramparts and rootless lava flows. During the intermediate and final eruptive stages (Roca Negra EU and Croscat EU, Fig. 6), in addition to spatter ramparts and lava flows, prolonged Hawaiian and Strombolian activity led to the construction of major, younger, cinder cones. The explosive activity of the youngest Croscat EU culminated with violent Strombolian activity of the Croscat Volcano, which constitutes the most explosive episode known for the central GVF (Cimarelli et al. 2010).

Cone morphology and morphotectonic features

Methodological approach

Cone morphology and morphotectonic features have been analysed through a dedicated geographic information system (GIS) based on a 5 m resolution DEM. The DEM is derived from the topographic maps of the Institut Cartografic de Catalunya (scale 1:5,000; contour interval 5 m).

The distribution of major morpho-structural features has been deduced by combining analysis of DEM-derived thematic maps such as slope, break in slope and slope aspect (horizontal direction to which the slope faces) with information from the drainage network map, following the methodology

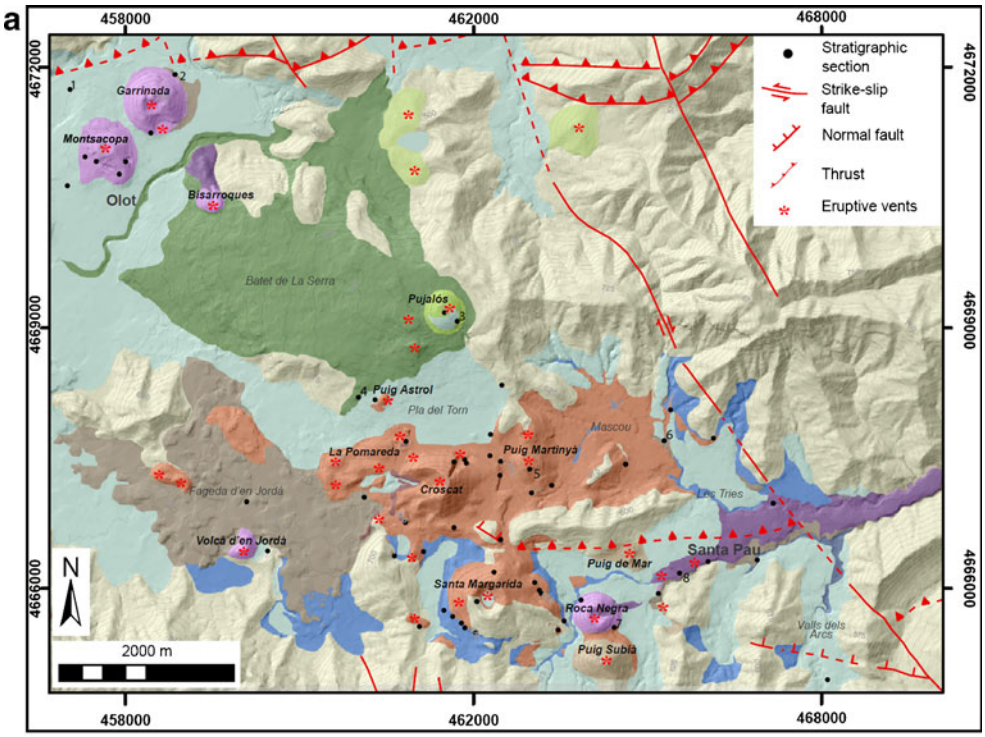

b

Synthems	Eruptive units	Epiclastic units	Eruptive centres	Lavas	Age
Les Tries		Upper Bosquet			
	Croscat		Croscat Pomareda Puig Astrol Santa Margarida	Can Xel F. d'en Jordà	11.5±1.1 ka 13.16/15.71 ky BP (*)
Mascou		Lower Bosquet			
	Roca Negra		Roca Negra Volcà d'en Jordà Garrinada Montsacopa Bisarroques	Upp. Santa Pau Bisarroques	28.1±2.6 ka
Santa Pau	Puig de Mar		Puig de Mar Puig Martinyà Puig Subià	Lower Santa Pau Les Tries Garrinada	110±30 ka 121±9.1 ka 132±12 ka
Valls dels Arcs		Valls dels Arcs			
	Batet de La Serra		Pujalós	Batet de La Serra	247±17 ka
		Pre-volcanic Basement			Paleocene - Eocene

Fig. 5 **a** Geological map of the central GVF area (descriptions and geometry of the Eocene rocks from IGC, 2002, 2003); **b** legend of the geological map and geochronology from the literature (Guérin et al. 1985). *Asterisk* refers to ^{14}C dates from Puiguriguer et al. 2012

described in Cimarelli and de Rita (2006). In order to deduce the main morpho-structural trends of the pre-volcanic basement rocks, this analysis was performed on an area that extends beyond the volcanic deposits. The frequency of the measured lineament azimuth was plotted on rose diagrams (Fig. 7).

Information on the orientation of magma-feeding fractures has been obtained for 15 eruptive centres through morphometric investigations (Table 3), following the methodology proposed by Corazzato and Tibaldi (2006). The main morphological parameters used in this analysis are the alignment of the coeval eruptive centres, elongation of the cones, alignment of

Table 1 Summary of the lithofacies characteristics of the recognised eruptive units

Units	Description	Eruptive vents or source	Interpretation
Clot Sagalla Unit	Bedding: absent Texture and grading: massive, chaotic, matrix-supported Clast size: sandy matrix (40 %); pebble clasts (60 %) Clast type: altered volcanic ashy-matrix; lava lithics and red spatter-type scoria Clast shape: sub-angular and platy-shaped Welding: absent Lithics/xenoliths: absent		Deposits of the Croscat volcano western flank
Can Xel Lava	Structure: massive to brecciated Texture: weakly porphyritic Phenocrysts: ol, cpx and plg	Croscat scoria cone	Effusive activity
Can Barraca Unit	Bedding: planar or low-angle cross-bedded, 10 cm-thick beds (proximal phreatomagmatic); cross- and planar-bedded, 1 to 5 cm-thick beds (medial and distal CMU reworked) Texture and grading: each bed is normal graded in proximal preatomagmatic deposits to reverse-graded (medial and distal reworked CMU deposits) Clast size: fine to coarse ash (both in proximal and in distal deposits) Clast type: moderate to highly vesicular scoriae Clast shape: blocky to highly stretched clasts Welding: absent Lithics/xenoliths: lava lithics	Croscat scoria cone	Deposits of pulsatory phreatomagmatic explosions and syn-CMU reworked material
Can Martinyà Unit	Bedding: planar, locally lenticular (proximal); planar (distal) Texture and grading: reverse to normal graded (both in proximal and in distal deposits) Clast size: lapilli, with bomb lenses (proximal); lapilli to coarse ash (distal) Clast type: moderately to highly vesicular scoriae: dense bombs are also present Clast shape: irregular to highly stretched clasts Welding: absent Lithics/xenoliths: high-silica glass-bearing xenoliths (Buchites)	Croscat scoria cone	Fall-out deposits from violent Strombolian explosions
Upper Quesito Unit	Bedding: mainly lenticular. Stratified, 20 mm-thick beds Texture and grading: multiple reverse grading Clast size: lapilli, bomb to lapilli Clast type: moderate vesicular scoriae Clast shape: aerodynamic shape of bomb clasts, irregular shape of lapilli clasts Welding: local moderate welding Lithics/xenoliths: rare Eocene calcarenitic xenoliths	Croscat scoria cone	Fall-out deposits from Strombolian explosions
Lower Quesito Unit	Bedding: mainly lenticular. Crudely stratified Texture and grading: massive to reverse grading Clast size: bomb, with minor lapilli Clast type: moderately vesicular scoriae and low vesicular spatter-type clasts	Croscat scoria cone; Pomareda spatter cone; Santa Margarida spatter cone; Puig Astrol spatter cone;	Fall-out deposits from Hawaiian-fountaining

Table 1 (continued)

Units	Description	Eruptive vents or source	Interpretation
	Clast shape: aereodynamic and fluidal shape, wrapping around underlying clasts	Undistinguished spatter cones	
	Welding: partially welded over much of deposit extent		
	Lithics/xenoliths: rare sanidine xenocrysts		
Can Caselles Unit	Bedding: planar, cross-bedded, 1 to 10 cm-thick beds (proximal); cross-bedded to planar-bedded, 1 to 10 mm-thick beds (distal)	Santa Margarida spatter cone	Dilute pyroclastc density current deposits from intermittent phreatomagmatic explosions
	Texture and grading: each bed is normal graded (both in proximal and in distal deposits)		
	Clast size: lapilli, fine to coarse ash (proximal); fine ash (distal)		
	Clast type: moderate to high vesicular scoriae		
	Clast shape: blocky to high-stretched clasts		
	Welding: absent		
	Lithics/xenoliths: abundant sandstones, marls and clacarenites; lava lithics are also present		
Upper Santa Pau Lava	Structure: massive to columnar jointed, sometimes pseudo-hyaloclastc. The base is brecciated	Roca Negra scoria cone	Effusive activity
	Texture: weakly porphyritic		
	Phenocrysts: ol, cpx and plg		
	Lithics/xenoliths: gabbroid, pyroxenitic and amphibolitic		
Roca Negra Unit	Bedding: mainly lenticular; stratified, 20–50-cm-thick beds	Roca Negra scoria cone	Fall-out deposits from Strombolian explosions
	Texture and grading: multiple reverse grading		
	Clast size: lapilli, bomb to lapilli		
	Clast type: moderate to dense vesicular scoriae		
	Clast shape: aerodynamic shape of bombs clasts, irregular shape of lapilli clasts		
	Welding: absent		
	Lithics/xenoliths: gabbroid, pyroxenitic and amphibolitic		
Volcà d'en Jordà	Bedding: mainly lenticular; stratified, 20–30-cm-thick beds	Volcà d'en Jordà scoria cone	Fall-out deposits from Strombolian explosions
	Texture and grading: multiple reverse grading		
	Clast size: lapilli, bomb to lapilli		
	Clast type: moderate vesicular scoriae		
	Clast shape: aerodynamic shape of bomb clasts, irregular shape of lapilli clasts		
	Welding: local moderate welding		
	Lithics/xenoliths: absent		
La Cambrafosca	Bedding: mainly lenticular; stratified, 10–20-cm-thick beds	La Cambrafosca eruptive vents	Fall-out deposits from Strombolian explosions
	Texture and grading: multiple reverse grading		
	Clast size: lapilli, bomb to lapilli		
	Clast type: moderate vesicular scoriae		
	Clast shape: aerodynamic shape of bomb clasts, irregular shape of lapilli clasts		
	Welding: local moderate welding		
	Lithics/xenoliths: Eocene sedimentary blocks		

Table 1 (continued)

Units	Description	Eruptive vents or source	Interpretation
Upper Garrinada	Bedding: mainly lenticular; massive to broadly stratified, 100–200-mm-thick beds Texture and grading: massive, mainly chaotic Clast size: ashy matrix (60 %–20 %); lapilli clasts Clast type: low vesicular scoriae Clast shape: angular clasts Welding: no welding, cohesive Lithics/xenoliths: crystal-rich ash matrix; very abundant cm-sized black lava, grey altered lava and calcarenitic clasts	La Garrinada scoria cone	Pyroclastic density current and fall-out deposit from phreatomagmatic/phreatic explosions
Lower Garrinada	Bedding: mainly lenticular; stratified, 30–50-cm-thick beds (LGU1); planar to cross-bedded, 1–10-cm-thick beds (LGU2) Texture and grading: multiple reverse grading (LGU1); alternate (LGU2) Clast size: bomb to lapilli (LGU1); lapilli and ash (LGU2) Clast type: moderate to vesicular scoriae (both LGU1 and LGU2) Clast shape: irregular shape clasts (LGU1); irregular to blocky shaped particles, with frequent palagonitisation (LGU2) Welding: absent Lithics/xenoliths: lava lithics	La Garrinada scoria cone	Fall-out deposits from Strombolian explosions (LGU1); fall-out and dilute pyroclastic density current from phreatomagmatic explosions
Upper Montsacopa	Bedding: cross-bedded, 50 to 200-mm-thick beds (proximal); cross-bedded to planar-bedded, 10- to 50-mm-thick beds (distal) Texture and grading: each bed is normal graded (both in proximal and distal deposits) Clast size: lapilli to coarse ash (proximal); fine to coarse ash (distal) Clast type: moderately to highly vesicular scoria Clast shape: blocky to highly stretched clasts Welding: absent Lithics/xenoliths: lava lithics	Montsacopa scoria cone	
Lower Montsacopa	Bedding: mainly lenticular; stratified, 20–50-cm-thick beds Texture and grading: multiple reverse grading Clast size: lapilli, bomb to lapilli Clast type: moderately to densely vesicular scoria Clast shape: aerodynamic shape of bomb clasts, irregular shape of lapilli clasts Welding: absent Lithics/xenoliths: gabbroid, pyroxenitic and amphibolitic	Montsacopa scoria cone	Fall-out deposits from Strombolian explosions
Bisarroques Lava	Structure: Clastogenic Texture: weakly porphyritic Phenocrysts:ol, cpx and plg Lithics/xenoliths: absent	Bisarroques spatter cone	Agglutination and flow of hot juvenile fragments from Hawaiian fountaining
Bisarroques Unit	Bedding: mainly lenticular, crudely stratified Texture and grading: massive to reverse grading	Bisarroques spatter cone	Fall-out deposits from Hawaiian-fountaining

Table 1 (continued)

Units	Description	Eruptive vents or source	Interpretation
	Clast size: bomb, with scarce lapilli Clast type: moderately vesicular scoria and weakly vesicular spatter-type clasts Clast shape: aerodynamic and fluidal shape, wrapping around underlying clasts Welding: partially welded over most of the deposit extent Lithics/xenoliths: absent		
Fageda d'en Jordà Phase	Structure: lava mounds, massive to jointed (both columnar and radial jointing) Texture: weakly porphyritic Phenocrysts: ol, cpx and plg Lithics/xenoliths: absent	Eruptive fissures in the Fageta d'en Jordà area	Large effusive activity
Lower Santa Pau Lava	Structure: massive to columnar jointed; the base is brecciated Texture: weakly porphyritic Phenocrysts: ol, cpx and plg Lithics/xenoliths: absent	Eruptive fissures between Puig the Mar spatter cone and Volcà d'en Simò spatter cone	Effusive activity
Les Tries Lava	Structure: massive to columnar jointed; the base is brecciated Texture: weakly porphyritic Phenocrysts: ol, cpx and plg Lithics/xenoliths: absent	Eruptive fissures near Puig de Martinyà area	Effusive activity
Garrinada Lava	Structure: massive to columnar jointed; the base is brecciated Texture: weakly porphyritic Phenocrysts:ol, cpx and plg Lithics/xenoliths: absent	Eruptive fissure in the Montsacopa–Garrinada area	Effusive activity
Les Cases Noves Unit	Bedding: mainly lenticular Texture and grading: massive, mainly chaotic Clast size: ashy matrix (90 %–60 %); lapilli clasts Clast type: moderate vesicular scoriae Clast shape: angular to irregular clasts Welding: absent, cohesive Lithics/xenoliths: centimetre-sized black lava, grey altered lava, calcarenite and marl clasts	Source in the Puig de Mar–Volcà d'en Simò area	Syn-eruptive reworked deposits
Puig de Mar Phase	Bedding: mainly lenticular, crudely stratified Texture and grading: massive to reverse grading Clast size: bomb, with minor lapilli Clast type: moderate vesicular scoriae and low vesicular spatter-type clasts Clast shape: aerodynamic and fluidal shape, wrapping around underlying clasts Welding: partially welded over most of deposit extent Lithics/xenoliths: rare sanidine xenocrysts	Puig de Mar spatter cone; Puig de Martinyà spatter cone; Volcà d'en Simò spatter cone; Puig Subià spatter cone; Undistinguished spatter cones	Fall-out deposits from Hawaiian-fountaining
Pujalos phase	Bedding: mainly lenticular. Crudely stratified Texture and grading: massive to reverse grading Clast size: bomb, with scarce lapilli Clast type: moderately vesicular scoria and weakly vesicular spatter-type clasts	Pujalos spatter cone; Undistinguished spatter cones	Fall-out deposits from Hawaiian-fountaining

Table 1 (continued)

Units	Description	Eruptive vents or source	Interpretation
	Clast shape: aerodynamic and fluidal shape, wrapping around underlying clasts		
	Welding: partially welded over most of deposit extent		
	Lithics/xenoliths: absent		
Batet de La Serra Lava	Structure: massive to columnar jointed; the base is brecciated	Eruptive fissures in the Batet de La Serra high-plain, near Pujalos spatter cone	Large effusive activity
	Texture: weakly porphyritic		
	Phenocrysts: ol, cpx and plg		
	Lithics/xenoliths: absent		

depressed sectors at the crater rim and the azimuth of breached sectors of the cones. Alignment of coeval cones, cone elongation and alignment of crater-rim depressed points are used as indicators of the direction of the feeding-fracture in the substrate, while cone breaching can either coincide with the weakest zone of the edifice or with the direction of maximum stress applied to its flanks by magma bulging or fracture propagation (Corazzato and Tibaldi 2006; Bonali et al. 2011). Alignment of volcanic centres has been assessed using Fry spatial distribution analysis. This method has been used to

Table 2 Summary of the lithofacies characteristics of the reworked deposits

Type of reworked deposit	Facies description
Syn-eruptive	Bedding: lenticular
	Texture and grading: massive, chaotic to reverse graded, clast-supported
	Clast size: ash to bombs and blocks
	Clast type: fresh to altered juvenile clasts (monomictic); lava lithics; crystals
	Clast shape: sub-angular
Early post-eruptive	Bedding: lenticular to low angle cross-bedded (proximal to the source), planar to low-angle cross bedded (medial to distal from the source)
	Texture and grading: massive to reverse graded, clast- to matrix-supported
	Clast size: ash to lapilli
	Clast type: altered to fresh juvenile clasts (monomictic); lava lithics; crystals
	Clast shape: sub-angular
Late post-eruptive	Bedding: lenticular to low angle cross-bedded (proximal to the source), planar to low-angle cross bedded (medial to distal from the source)
	Texture and grading: massive to reverse graded, clast- to matrix-supported
	Clast size: sand and pebbles
	Clast type: altered juvenile clasts (polymictic); lava lithics; Eocene sedimentary clasts (rare or concentrated in lenses)
	Clast shape: sub-angular to sub-rounded
Inter-eruptive	Bedding: not bedded, lenticular to low angle cross-bedded
	Texture and grading: massive, chaotic or reverse to normal graded, clast- to matrix-supported
	Clast size: sand and pebbles (near the source), sand and silt (plain facies)
	Clast type: Eocene sedimentary clasts, altered juvenile clasts (polymictic); lava lithics
	Clast shape: sub-rounded to sub-angular

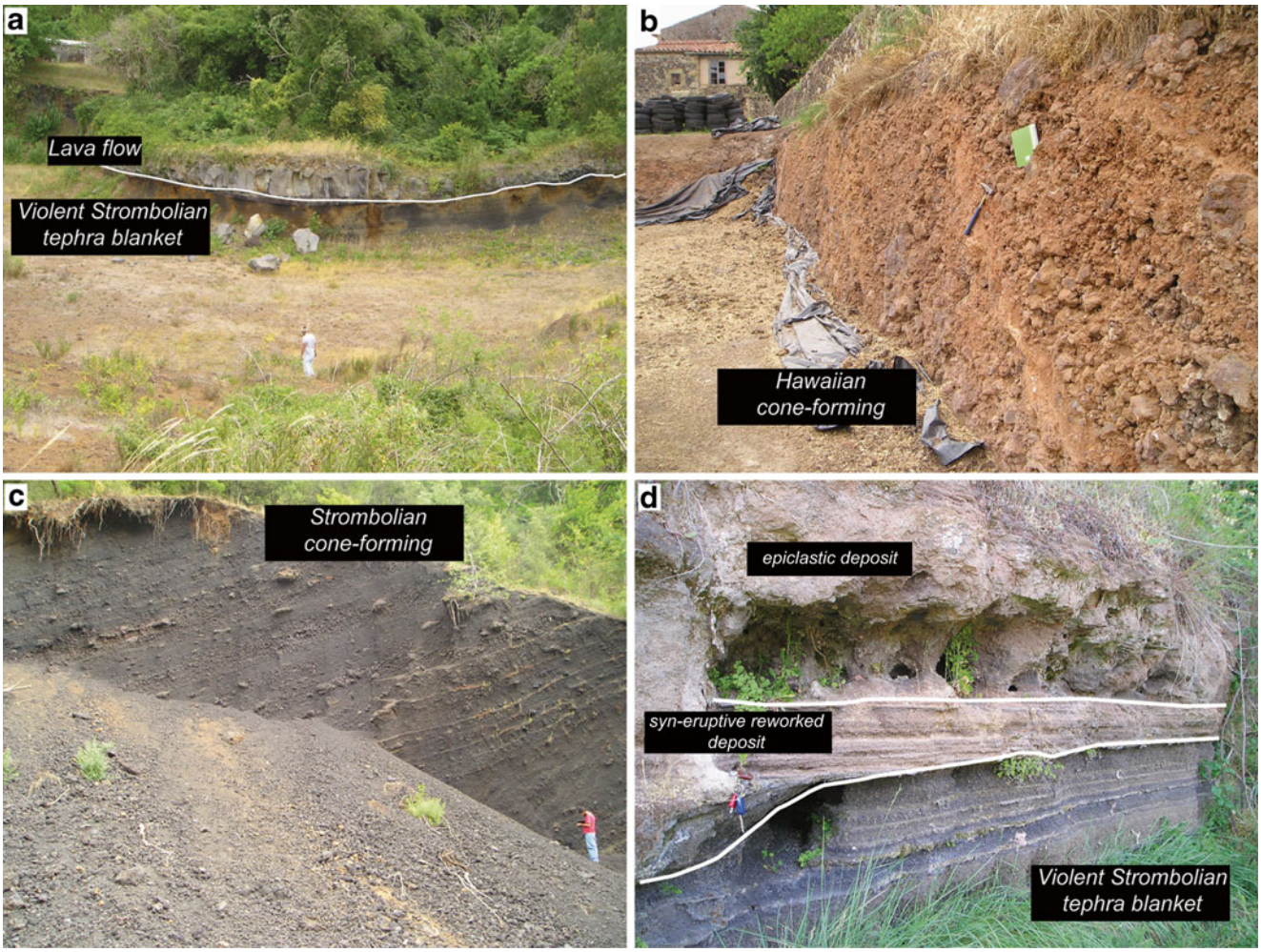

Fig. 6 Different facies in primary deposits: **a** massive to well-laminated, lapilli to ash scoria blanket (Violent Strombolian style, Croscat EU) topped by columnar-jointed lava; **b** welded bombs and spatter agglomerates of the Puig de Mar EU, produced during Hawaiian-style lava fountaining; **c** bedded scoria deposits of the Roca Negra EU (Roca Negra scoria cone), produced during Strombolian-type eruptions; **d** massive to well-bedded, lapilli to ash scoria blanket (Violent Strombolian style, Croscat EU), topped with wavy-bedded scoria-rich sand (post-eruptive reworking) and massive sand with lenses of pebbles from Eocene deposits (inter-eruptive reworking)

determine strain form the distribution of objects in a rock (Fry 1979) and preferred orientation of volcanic cone alignments (Gutiérrez et al. 2005).

Morphological analysis

Our statistical analysis of morphological lineaments in the pre-volcanic basement reveals three main populations of NW-, N- and NE-striking features (Fig. 7a). The most representative NW-striking features are oriented according to the direction of the main transtensional faults limiting the tectonic depression (Amer and Llorát faults). Analysis of the hydrographic features shows that streamlines ≥700 m are scattered in all directions with the main populations represented by E-, NW-, N- and NE-oriented elements (Fig. 7b and B1). With respect to the morpho-structural lineaments of the substrate, the additional E-trending population accounts for the elements incising the volcanic deposits. Here, volcanic deposits masked the underlying morphology of the substrate and forced the drainage system to rearrange accordingly. When restricting the analysis to hydrographic features ≥800 m, the resulting rose-diagram further highlights this effect (Fig. 7, B2).

Investigations of the spatial distribution and morphology of cones provided information on the stress tensor driving the emplacements of feeder dikes and their interaction with pre-existing fractures in the basement. Both alignment of depressed sectors of crater rims and the spatial distribution of eruptive centres reveal NNW- to NW-striking eruptive fractures (Fig. 7c, d; Table 3). Alignments of coeval eruptive centres also show ENE to NE directions, as in the case of the Garrinada-Montsacopa-Montolivet cones. It is worth noting that the azimuths of the breaching sectors are oriented orthogonal to the eruptive fractures determined from the other three morphological parameters, which suggests that cone

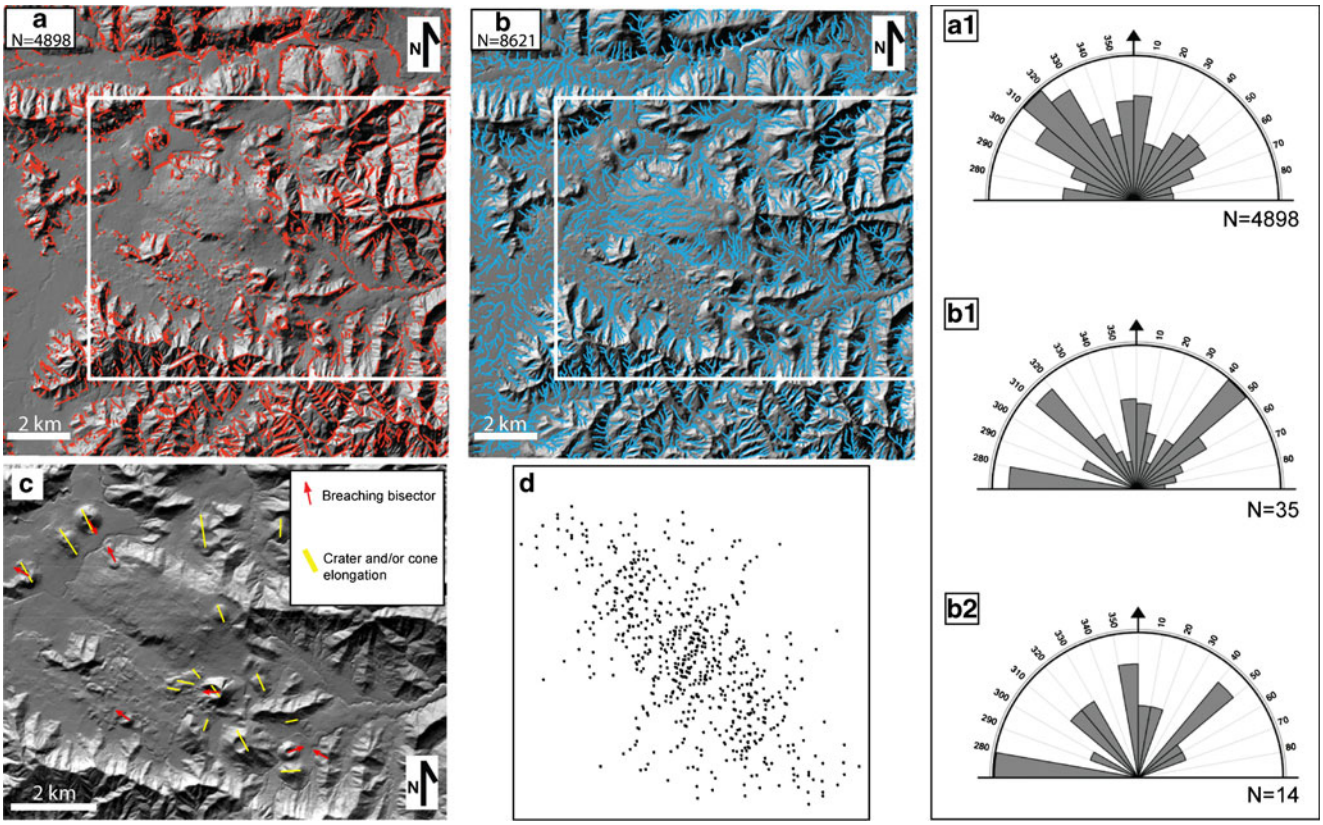

Fig. 7 DEM-derived maps of morphological elements: **a** morphotectonic lineaments and related rose diagram (A1); **b** drainage network elements; rose diagrams of hydrological elements ≥700 m (*B1*) and ≥800 m (*B2*); **c** direction of elongation (*yellow*) and breaching (*red*) of cones and craters; **d** fry plot describing the spatial distribution of the cones and their preferential alignments

breaching probably occurred by lava accumulation or bulging of cone flanks (Nolesini et al. 2013).

The volumes of ejecta in edifices have been determined by combining field measurements with the DEM analysis. The volume of each cone has been calculated using the DEM surface enclosed within its basal perimeter (defined using both slope maps and direct field observation), while lava flow volume was calculated by multiplying the flow area by the estimated mean thickness (Table 3). To better constrain changes in flow thickness, several longitudinal profiles were made following the methodology described by Rodriguez-Gonzalez et al. (2010).

Volumes of individual pyroclastic edifices vary from 10^6 to 10^8 m^3 dense rock equivalent (DRE). Major scoria cones (Croscat, Montsacopa and Garrinada), characterised by larger volumes and a volcanic succession dominated by lapilli and ash, are located near the depocentre of the tectonic depression, while the smaller ones, characterised by lower volumes and coarse-grained materials, are located near the valley margins and are associated with larger volume lava flows.

The Santa Margarida volcano is the only maar-type eruptive centre in the studied area. The thin deposits of this eruptive centre drape the partially excavated Eocene basement and are found intercalated in the eruptive succession of the nearby Croscat Volcano (Martí et al. 2011). As already reported by Di Traglia et al. (2009), the geometry and distribution of the deposits related to the Croscat EU indicate that volcanic activity occurred contemporaneously from multiple vents (Santa Margarida, Croscat, Pomareda and Puig Astrol) along a NNW-striking fracture.

Geometry and volume of the volcanic products

In order to estimate the volume of volcanic material in the central GVF, we modelled the top surface of the Eocene succession based on the stratigraphy of water wells (Custodio Gimena et al. 1984) and field data (Fig. 8). The volume of material between the topographic surface and the top Eocene surface was determined using the GIS by subtracting the elevations of the two surfaces. While the topographic surface is derived from the DEM, the top Eocene surface is interpolated using the stratigraphy of 28 wells intercepting that surface and using the limits of pre-volcanic outcrops as additional surface points (Fig. 8). The volumes of the major cones have also been subtracted, in order to highlight the depocentres in the pre-volcanic basement. Considering the negligible thickness of epiclastic material compared with that of the volcanic products,

Table 3 Morphometric parameters of the volcanic centres

Cone name	Croscat	Garrinada	Montsacopa	Puig Subià	Roca Negra	Puig Jordà	Pomareda
Cone volume ($\times 10^6$ m^3 DRE)	10.22	12	7.11	8.44	4.89	0,89	10.67
Tephra blanket volume ($\times 10^6$ m^3) DRE	13.66	None	0.8	None	None	None	None
Related lava flow volume ($\times 10^6$ m^3)	10	None	None	None	5.2	None	0
Total volume ($\times 10^6$ m^3 DRE)	33.88	12	7.91	8.44	10.09	0,89	10.67
Cone basal area (km^2)	0.74	0.53	0.35	0.3	0.2	0,6	0.55
Tephra dispersal area (km^2)	8	0.53	0.41	None	None	None	None
Related lava flow area (km^2)	0.05	None	None	None	1.04	None	0
Cone height (m)	189.04	128.03	97.17	144.35	110.2	63,42	31.38
Outer slope angle	25	26	23	23	28	25	20
Basement dip angle	0	0	0	<10	<10	<10	0
Max elong. axis length (m)		798	778	670			1255
Max elong. axis azimuth		N154	N135	N088			N057
Crater rim depressed point alignment		N334	N315				
Breaching direction	N267				N055	N295	
Cone name	Pujalos	Santa Margarida	Puig Astrol	Puig de Mar	Bisarroques	Sant Miquel Sacot	Puig Simò
Cone volume ($\times$106 DRE m^3)	1.78	1.78	0.04	1.69	0.27	0.22	0.18
Tephra blanket volume ($\times 10^6$ m^3 DRE)	None	None	None	None	None	None	None
Related lava flow volume ($\times 10^6$ m^3)	13.34	None	None	5.85	0.24	None	None
Total volume ($\times 10^6$ m^3 DRE)	15.12	1.78	0.04	7.54	0.51	0.22	0.18
Cone basal area (km^2)	0.13	0.11	0.01	0.12	0.04	0.02	0.02
Tephra dispersal area (km^2)	None	None	None	None	None	None	None
Related lava flow area (km^2)	6.67	None	None	1.17	0.12		None
Cone height (m)	59.51	80.78	30.93	77.41	49.33	48.55	39.77
Outer slope angle	18	24	20	25	19	20	15
Basement dip angle	<10	>10	10	<10	>10	>10	>10
Max elong. axis length (m)	516			581			
Max elong. axis azimuth	N167			73			
Crater rim depressed point alignment	N000						
Breaching direction					N347		N124

For the Santa Margarida volcano, only the morphometric parameters of the associated scoria rampart have been extrapolated

we estimate the total volume of the volcanics to be about 0.5 km^3 DRE.

This procedure allowed us to image the geometry of the sedimentary basin and to correlate thickness variations of the deposits with the distribution of the volcanic edifices within the tectonic depression.

The map of Fig. 8a shows two depressions where volcanic products are thicker: One corresponds to Olot village, while the other is located in the central sector of the tectonic depression beneath the Croscat volcano. The Olot village depression, where the Garrinada and Montsacopa scoria cones are located, hosts about 30 m of volcanic material, comprising lavas and subordinate pyroclastic deposits. The second depression (well constrained by water-well log data) extends roughly E-W and hosts about 160 m of volcanic products (Fig. 8b), thus identifying a basin depocentre near the Croscat-Pomareda cones. In both cases, the maximum thickness of volcanic deposits corresponds to the location of the major volcanic edifices of the central GVF.

Discussion

Temporal evolution of volcanic activity

According to the stratigraphy proposed here, each Eruptive Unit represents a series of eruptions clustered in time, occurring between 247±17 and 11.5±1.1 ka (Fig. 4; Guérin et al. 1985; Puiguriguer et al. 2012).

Although we carefully reconstructed the relative chronology of the eruptive products, existing geochronological data do not allow precise determination of the absolute duration of the eruptive and quiescent periods. We can infer that quiescence between the eruptive periods was long enough to allow the

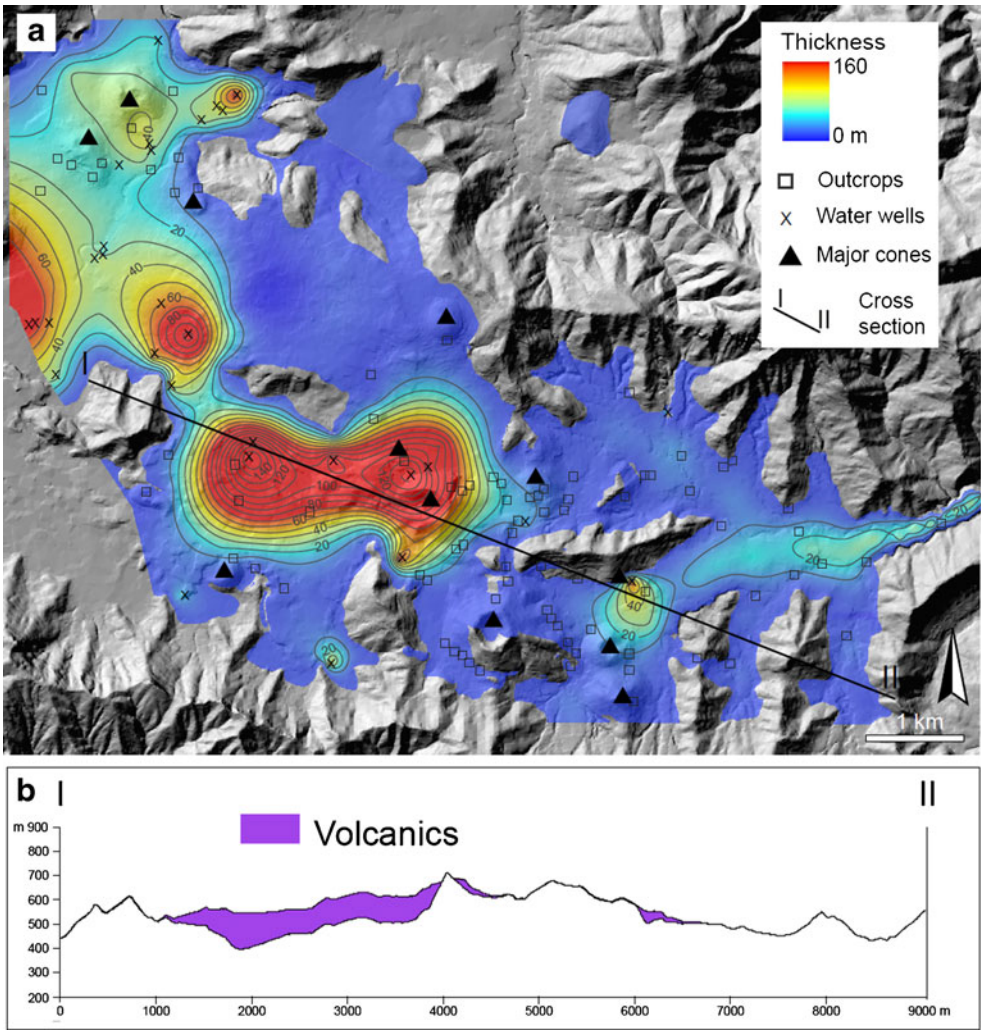

Fig. 8 **a** Isopach map of the volcanic and volcanoclastic deposits overlying the sedimentary basement. Two major depocentres are visible along the main axis of the Santa Pau-Olot valley. **b** Simplified geological section of the central GVF area showing the thickness of the volcanic deposits

formation of the decimetre-thick paleosols and metric erosive surfaces observed in the field (Fig. 3). In particular, given the unfavourable paleoclimatic conditions for mature soil formation, established during the Quaternary in the Pyrenees region (Pallàs et al. 2006), the thickness of the paleosols and the extent of the major erosive surfaces (S1) suggest quite a long interval of inactivity (of the order of tens of kyr based on the available datings; Guérin et al. 1985).

Recent radiocarbon dating of the paleosol contained in the Lower Bosquet Unit (Puiguriguer et al. 2012), coupled with the age (determined by thermoluminescence on plagioclase crystals) of the Upper Santa Pau lava in the upper Roca Negra EU (28.1±2.6 ka; Guérin et al. 1985) indicate quiescence of about 15 kyr between the two last eruptive units. The same calculation can be made for the time interval between Valls dels Arcs and Santa Pau synthems. Considering the age of the Batet de La Serra Lava (247±17 ka, Guérin et al. 1985) and Garrinada Lava (132±12 ka, Guérin et al. 1985), a quiescence of about 115 kyr can be estimated. The dating available for the Lower Santa Pau Lava (Puig de Mar EU) and the Upper Santa Pau Lava (Roca Negra EU) suggest a maximum duration of the Roca Negra EU of about 82 kyr.

Spatial evolution of the volcanic activity

Volcanic activity developed through time with progressive vent migration from the margin toward the centre of the tectonically controlled depression (Fig. 9). This migration is likely to have been favoured by a progressive symmetrical extension of the basin, as indicated by the distribution of maximum thickness of volcanic deposits along the axis of the Olot-Santa Pau valley. Cinder cones in the central GVF are aligned along NNW to NW and ENE to NE directions while morphological characteristics of the cones (cone and crater elongation) prevalently suggest that feeder dykes followed NW to NNW directions. This is in general agreement with the orientation of morphostructural lineaments of the pre-volcanic basement. Magma ascending into the crust is likely to be captured by shallow reactivated faults and fractures, therefore dykes might have near-surface orientations

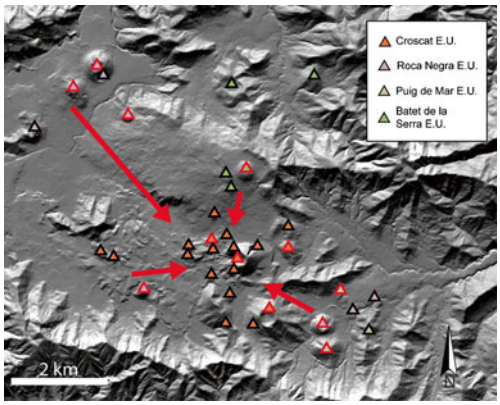

Fig. 9 Vent migration during emplacement of the four Eruptive Units. The oldest vents (Batet de La Serra EU and Puig de Mar EU) are located near the structural highs, while the youngest (Roca Negra EU and Croscat EU) are located at the centre of the tectonic depression

that are not simply perpendicular to the least principal stress direction (Connor and Conway 2000; Valentine and Perry 2007; Le Corvec et al. 2013). Our data show that, in the Central GVF, feeder dikes most probably intruded along pre-existing fractures of the substrate. It is interesting to note that the most recent volcano, Croscat EU, which also represents the peak of explosive activity, has been fed by dikes oriented NNW (Fig. 7), i.e. congruently with the orientation of the present stress tensor in the area (Goula et al. 1999).

Eruptive style and volcanic output rate

Migration of volcanism toward the centre of the basin coincided with a trend of increasing explosivity, as indicated by the characteristics of the deposits. The occurrence of progressively more explosive activity is characteristic of the volcanoes in the central part of the tectonic depression, where more complex and younger volcanic centres displaying violent Strombolian and phreatomagmatic activity are located. A shift in eruptive style from predominantly effusive and spatter-forming activity in the older and marginal eruptive vents (Batet de La Serra EU and Puig de Mar EU) to more complex and intense activity in the younger and central ones (Roca Negra EU and Croscat EU) is recorded in the stratigraphic succession and facies distribution of the deposits within the eruptive units. Younger eruptions exhibited a broader range of eruptive styles, as occurred during the Croscat eruption with the shift in eruptive intensity from Hawaiian–Strombolian to violent Strombolian (Di Traglia et al. 2009) and the occurrence of a phreatomagmatic episode at the contemporaneously active Santa Margarida volcano (Martí et al. 2011). The dynamics of this eruption, as compared with similar studied eruptions (Valentine et al. 2005; Pioli et al. 2008; Guilbaud et al. 2009) suggests a very high flux of gas-charged magma during this stage of volcanism. Phreatomagmatism occurred in volcanoes located on both high-transmissivity (Montsacopa, Garrinada) and low-transmissivity aquifers (Santa Margarida, Martí et al. 2011), without a specific correlation with aquifer permeability.

In order to estimate the magmatic input rate in the central GVF, we combined volumetric data of emitted products with the tectonic extension rate and the available geochronological datings. We plotted central GVF data (Fig. 10) on the differential-stress versus normalised output-rate diagram proposed by Takada (1994). We used the 0.05–0.125 mm/year vertical slip rate deduced by Fleta et al. (2001) for the Amer fault as an order of magnitude estimate of the differential stress in the studied area during the Quaternary. The results show that the GVF can be classified as a low output rate/small differential stress volcanic field characterised by low average volume of products emitted during each eruptive cluster and by long periods of quiescence between them.

Conclusive remarks

We investigated the geological and morphological evolution of the central area of the Garrotxa Volcanic Field and determined the relationship between eruptive styles and volcano distribution through time within the central Garrotxa tectonic depression.

The main outcomes of this study can be summarised as follows:

– Each recognised synthem bounded by major unconformities (S1) comprises the primary products of volcanic activity and their syn-eruptive reworked deposits (Eruptive Units) and of products of erosion and re-deposition processes (Epiclastic Units). The time period separating eruptive and syn-eruptive deposition from the widespread erosion and deposition of epiclastic material is represented by the S2 unconformity surfaces. The quiescence between two eruptive units is represented in the GVF stratigraphic record by the

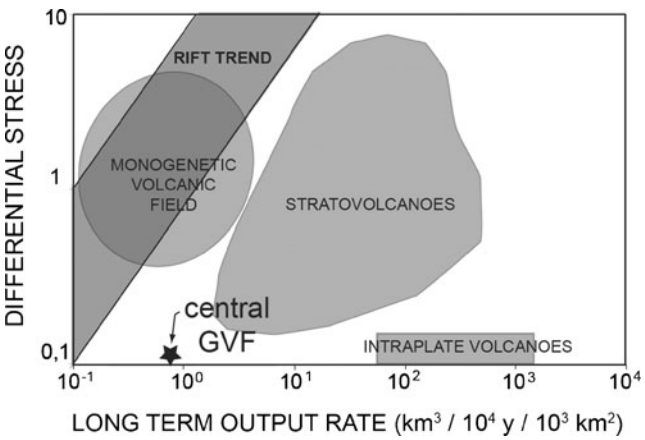

Fig. 10 Differential-stress data versus normalised output-rate plot (following Takada 1994). GVF can be classified as a low-output rate, tectonically controlled volcanic field, the activity of which is mainly controlled by tectonics in the NE Catalunya region (stress value from Fleta et al. 2001)

unconformities produced by erosion or by the sedimentary (epiclastic) deposits, bounded at the bottom and at the top by S2 and S1 unconformities, respectively. The eruptive units represent the products of one or more eruptions clustered in time separated by time-breaks long enough to produce significant unconformities (S3 surfaces).

- The morphology and alignments of cinder cones in the studied area suggest that feeder dykes followed the orientation of local structural features formed in response to the active stress tensor which characterises the strike-slip tectonic regime active in the NEVP since the Pliocene–Pleistocene.
- The facies characteristics and distribution of deposits shows that migration of volcanism toward the centre of the basin coincided with a trend of increasing explosivity through time. Phreatomagmatism occurred without a specific geographic correlation and independently from the permeability characteristics of the aquifer underlying the eruptive centres.
- Given the small average volume of products emitted during each eruptive cluster and the long quiescence between them (15 and 115 kyr), the GVF can be classified as a low output rate/small differential stress volcanic field.
- The use of the UBSU stratigraphy in volcanic terrains is confirmed as a powerful tool for unravelling the spatial and temporal evolution of volcanic systems. In particular, the versatility of this methodology based on the recognition of surfaces with relative hierarchy allows its application to volcanic areas of different geographic extents. Use of UBSU is particularly effective for basaltic monogenetic volcanic fields in which the homogeneous chemical composition of deposits makes the use of petro-chemical mapping criteria ineffective.
- In the absence of tephra layers suitable for establishing a tephrostratigraphic framework, correlation of widely extended unconformity surfaces made possible the stratigraphic correlation between widely spaced and low-output rate volcanic centres in this volcanic field.

Acknowledgements The authors are grateful to the Parc Natural de la Zona Volcanica de la Garrotxa for logistical support. We thank G. Gisbert and M. Aulinas for photos and assistance during the fieldwork and also M.N. Gibauld, A. Tibaldi and J.D.L. White for insightful and constructive review of the manuscript. This research was carried out in the framework of the Research Group PEGEFA (SGR-2005-795; AGAUR, DURSI de la Generalitat de Catalunya) and partially funded by the Project CGL2007-63727/BTE of the Spanish Ministry of Education and Science. F.DiT. benefited of a mobility scholarship from Università degli Studi Roma Tre.

References

Araña V, Aparicio A, Martìn C, Garcìa L, Ortiz R, Vaquer R, Berberi F, Ferrara G, Albert J, Gassiot X (1983) El vulcanismo neògeno—cuaternario de Cataluña: Caracteres estructurales, petrològicos y geodinàmicos. Acta Geol Hisp T.18(1):1–17

Bianchini G, Beccaluva L, Bonadiman C, Nowell G, Pearson G, Siena F, Wilson M (2007) Evidence of diverse depletion and metasomatic events in harzburgite-lherzolite mantle xenoliths from the Iberian plate (Olot, NE Spain): implications for lithosphere accretionary processes. Lithos 94:25–45. doi:10.1016/j.lithos.2006.06.008, ISSN 0024–4937

Bonali F, Corazzato C, Tibaldi A (2011) Identifying rift zones on volcanoes: an example from La Réunion Island, Indian Ocean. Bull Volcanol 73:347–366

Carracedo Sánchez M, Sarrionandia F, Arostegui J, Eguiluz L, Gil Ibarguchi JI (2012) The transition of spatter to lava-like body in lava fountain deposits: features and examples from the Cabezo Segura volcano (Calatrava, Spain). J Volcanol Geotherm Res 227–228:1–14

Cebrià JM, López–Ruiz J, Doblas M, Oyarzun R, Hetogen J, Benito R (2000) Geochemestry of the Quaternary alkali basalts of Garrotxa (NE Volcanic Province, Spain): a case of double enrichment of the mantle lithosphere. J Volcanol Geotherm Res 102:217–235

Cimarelli C, de Rita D (2006) Structural evolution of the Pleistocene Cimini trachytic volcanic complex (Central Italy). Bull Volcanol 68: 538–548

Cimarelli C, Di Traglia F, Taddeucci J (2010) Basaltic scoria textures from a zoned conduit as precursors to violent Strombolian activity. Geology 38:439–442. doi:10.1130/G30720.1

Condit CD, Connor CB (1996) Recurrence rates of volcanism in basaltic volcanic fields: an example from the Springerville Volcanic Field, Arizona. Geol Soc Am Bull 108:1225–1241

Connor CB, Conway FM (2000) Basaltic volcanic fields. In: Sigurdsson H, Houghton BF, McNutt SR, Rymer H, Stix J (eds) Encyclopedia of volcanoes. Academic Press, San Diego, pp 331–343

Corazzato C, Tibaldi A (2006) Fracture control on type, morphology and distribution of parasitic volcanic cones: an example from Mt. Etna, Italy. J Volcanol Geotherm Res 158:177–194

Custodio Gimena E, Vifials E, Pascual JM, Bayò, A, Domenech J (1984) Plan Hidrològico del Pirineo Oriental: Area de Olot-Alto Fluvià. Confederaciòn Hidrográfica del Pirineo Oriental, unpubl, rep., 46 pp

de Rita D, Giordano G, Milli S (1997) Forestepping-backstepping stacking pattern of volcaniclastic successions: Roccamonfina volcano, Italy. J Volcanol Geotherm Res 78:267–288. doi:10.1016/S0377-0273(97)00005-X

Di Traglia F, Cimarelli C, de Rita D, Gimeno Torrente D (2009) Changing eruptive styles in basaltic explosive volcanism: examples from Croscat complex scoria cone, Garrotxa Volcanic Field (NE Iberian Peninsula). J Volcanol Geotherm Res 180:89–109. doi:10.1016/j.jvolgeores.2008.10.020

Di Traglia F, Pistolesi M, Rosi M, Bonadonna C, Fusillo R, Roverato M (2013) Growth and erosion: the volcanic geology and morphological evolution of La Fossa (Island of Vulcano, Southern Italy) in the last 1000 years. Geomorphology 194:94–107

Dóniz J, Romero C, Coello E, Guillén C, Sánchez N, García-Cacho L, García A (2008) Morphological and statistical characterisation of recent mafic volcanism on Tenerife (Canary Islands, Spain). J Volcanol Geotherm Res 173:185–195

Donville B (1976) Géologie Neogène de la Catalogne Orientale. Bull. B.R.G.M., 2ème serie, Sect. IV, 177 – 210

Fisher RV, Schmincke H-U (1984) Pyroclastic rocks. Springer–Verlag, Berlin

Fleta J, Santanach P, Martínez P, Grellet B, Masana E (2001) Preliminary geologic, geomorphologic and geophysical studies for the paleoseismological analysis of the Amer fault (NE Spain). Neth J Geosci 80:243–253

Fry N (1979) Random point distribution and strain measurement in rocks. Tectonophysics 60:89–105

Gallart J, Pous J, Boix F, Hirn A (1991) Geophysical constraints on the crustal structure of the Olot Volcanic area, NE of the Iberian Peninsula. J Volcanol Geotherm Res 47:33–44

Gimenez-Monsant J, Calvet F, Tucker ME (1999) Silica diagenesis in Eocene shallow-water platform carbonates, southern Pyrenees. Sedimentology 46:969–984

Gisbert Pinto G, Gimeno Torrente D, Fernandez-Turiel JL (2009) Eruptive mechanisms of the Puig de La Garrinada volcano (Olot, Garrotxa Volcanic Province, Northeastern Spain): a methodological study developed on proximal pyroclastic deposits. J Volcanol Geotherm Res 180:259–276

Goula X, Olivera C, Fleta J, Grellet B, Lindo R, Rivera LA, Cisternas A, Carbon D (1999) Present and recent stress regime in the eastern part of the Pyrenees. Tectonophysics 308:487–502

Guérin G, Behamoun G, Mallarach JM (1985) Un exemple de fusió parcial en medi continental. El vulcanisme quaternari de la Garrotxa. Vitrina, Museu Comarcal de la Garrotxa, nº 1, pp 19–26

Guilbaud MN, Siebe C, Agustín-Flores J (2009) Eruptive style of the young high-Mg basaltic-andesite Pelagatos scoria cone, southeast of México City. Bull Volcanol 71:859–880. doi:10.1007/s00445-009-0271-0

Gutiérrez F, Gioncada A, González Ferran O, Lahsen A, Mazzuoli R (2005) The Hudson Volcano and surrounding monogenetic centres (Chilean Patagonia): an example of volcanism associated with ridge–trench collision environment. J Volcanol Geotherm Res 145:207–233

Head JW, Wilson L (1989) Basaltic pyroclastic eruptions: influence of gas-release patterns and volume fluxes on fountain structure, and the formation of cinder cones, spatter cones, rootless flows, lava ponds and lava flows. J Volcanol Geotherm Res 37:261–271

IGC (Institut Geològic de Catalunya). (2002) Cartografia Temàtica. Sèrie Mapa Geològic de Catalunya. Santa Pau. Available at http://www1.igc.cat/web/gcontent/pdf/mapes/igc_GT1_295q11_75x23_v1g.pdf

IGC (Institut Geològic de Catalunya). (2003) Cartografia Temàtica. Sèrie Mapa Geològic de Catalunya. Olot. Available at http://www1.igc.cat/web/gcontent/pdf/mapes/igc_GT1_257q12_75x22_v1g.pdf

Keating GN, Valentine GA, Krier DJ, Perry FV (2008) Shallow plumbing systems for small-volume basaltic volcanoes. Bull Volcanol 70:563–582. doi:10.1007/s00445-007-0154-1

Kiyosugi K, Connor CB, Zhao D, Connor LJ, Tanaka K (2010) Relationships between volcano distribution, crustal structure, and P-wave tomography: an example from the Abu Monogenetic Volcano Group, SW Japan. Bull Volcanol 72:331–340. doi:10.1007/s00445-009-0316-4

Le Corvec N, Spörli KB, Rowland J, Lindsay J (2013) Spatial distribution and alignments of volcanic centers: clues to the formation of monogenetic volcanic fields. Earth-Sci Rev 124:96–114. doi:10.1016/j.earscirev.2013.05.005

Lewis C, Vergés J, Marzo M (2000) High mountains in a zone of extended crust: insights into the Neogene–Quaternary topographic development of northeastern Iberia. Tectonics 19:86–102

Martí J, Mitjavila J, Roca E, Aparicio A (1992) Cenozoic magmatism of the Valencia trough (Western Mediterranean): relationship between structural evolution and volcanism. Tectonophysics 203:145–165

Martí J, Planaguma L, Geyer A, Canal E, Pedrazzi D (2011) Complex interaction between Strombolian and phreatomagmatic eruptions in the Quaternary monogenetic volcanism of the Catalan Volcanic Zone (NE of Spain). J Volcanol Geotherm Res 201(1–4):178–193. doi:10.1016/j.jvolgeores.2010.12.009

Mauffret A, Pascal G, Maillard A, Gorini C (1995) Tectonics and deep structure of the north-western Mediterranean Basin. Mar Petrol Geol 12:645–666

Mertes H, Schmincke H-U (1985) Mafic potassic lavas of the Quaternary West Eifel volcanic field. Contrib Mineraletrol 89:330–345

Nolesini T, Di Traglia F, Del Ventisette C, Moretti S, Casagli N (2013) Deformations and slope instability on Stromboli volcano: integration of GBInSAR data and analogue modeling. Geomorphology 180–181: 242–254

Pallàs R, Rodés A, Braucher R, Carcaillet J, Ortuño M, Bordonau J, Bourlès D, Vilaplana JM, Masana E, Santanach P (2006) Late Pleistocene and Holocene glaciation in the Pyrenees: a critical review and new evidence from 10Be exposure ages, south-central Pyrenees. Quat Sci Rev 25:2937–2963

Parfitt E (2004) A discussion of the mechanisms of explosive basaltic eruptions. J Volcanol Geotherm Res 134:77–107

Pioli L, Erlund E, Johnson E, Cashman K, Wallace P, Rosi M, Delgado Granados H (2008) Explosive dynamics of violent Strombolian eruptions: the eruption of Parícutin Volcano 1943–1952 (Mexico). Earth Planet Sci Lett 271:359–368

Puiguriguer M, Alcalde G, Bassols E, Burjachs F, Expósito I, Planagumà L, Saña M, Yll E (2012) ^{14}C dating of the last Croscat volcano eruption (Garrotxa Region, NE Iberian Peninsula). Geol Acta 10: 43–47

Rodriguez-Gonzalez A, Fernandez-Turiel JL, Perez-Torrado FJ, Gimeno D, Aulinas M (2010) Geomorphological reconstruction and morphometric modelling applied to past volcanism. Int J Earth Sci 99: 645–660

Salvador A (1987) Unconformity-bounded stratigraphic units. Geol Soc Am Bull 98:232–237

Salvador (1994) International Stratigraphic Guide. A guide to stratigraphic classification, terminology and procedure, Edited by The International Union of Geological Sciences and The Geological Society of America

SGC (Servei Geològic de Catalunya) (1989) Mapa Geològic de Catalunya escala 1:250.000. Generalitat de Catalunya

Takada A (1994) The influence of regional stress and magmatic input on styles of monogenetic and polygenetic volcanism. J Geophys Res 99(B7):563–573

Tibaldi A (1995) Morphology of pyroclastic cones and tectonics. J Geophys Res 100(B12):24521–24535

Valentine GA, Gregg TKP (2008) Continental basaltic volcanoes—processes and problems. J Volcanol Geotherm Res 177:857–873. doi:10.1016/j.jvolgeores.2008.01.050

Valentine G, Hirano N (2010) Mechanisms of low-flux intraplate volcanic fields—basin and range (North America) and northwest Pacific Ocean. Geology 38:55–58. doi:10.1130/G30427.1

Valentine GA, Keating GN (2007) Eruptive styles and inferences about plumbing systems at Hidden Cone and Little Black Peak scoria cone volcanoes (Nevada, U.S.A.). Bull Volcanol 70:104–113. doi:10.1007/s00445-007-0123-8

Valentine G, Perry F (2007) Tectonically controlled, time-predictable basaltic volcanism from lithospheric mantle source. Earth Planet Sci Lett 261:201–216

Valentine GA, Krier D, Perry FV, Heiken G (2005) Scoria cone construction mechanisms, lathrop wells volcano, southern Nevada, USA. Geology 33:629–632. doi:10.1130/G21459

Vergés J, Sàbat F (1999) Constraints on the western Mediterranean kinematics evolution along a 1,000-km transect from Iberia to Africa., in Durand, B., Jolivet, L., Horvath, F., and Séranne, M., eds., The Mediterranean basins: Tertiary extension within the Alpine orogen. Geochem Soc Spec Publ 156:63–80

Walker GPL (1993) Basaltic-volcano system. In Magmatic process and plate tectonics, Geological Society, London, Special Publication, 76, 3–3

Wilson M, Downes H, Cebrià JM (1995) Contrasting fractionation trends in coexisting continental alkaline magma series; Cantal, Massif Central, France. J Petrol 36:1729–1753

Zeyen HJ, Banda E, Klingelé E (1991) Interpretation of magnetic anomalies in the volcanic area of north-eastern of Spain. Tectonophysics 192:201–210